

Superconducting effects in optimization of magnetic penetration thermometers for x-ray microcalorimeters

T.R. Stevenson, M.A. Balvin, S.R. Bandler, S.E. Busch, K.L. Denis, W.-T. Hsieh, D.P. Kelly, W. Merrell, P.C.

Nagler, J.-P. Porst, J.E. Sadleir, G.M. Seidel, S.J. Smith

Abstract: We have made high-resolution x-ray microcalorimeters using superconducting MoAu bilayers and Nb meander coils. The temperature sensor is a Magnetic Penetration Thermometer (MPT). Operation is similar to metallic magnetic calorimeters, but instead of the magnetic susceptibility of a paramagnetic alloy, we use the diamagnetic response of the superconducting MoAu to sense temperature changes in an x-ray absorber. Flux-temperature responsivity can be large for small sensor heat capacity, with enough dynamic range for applications. We find models of observed flux-temperature curves require several effects to explain flux penetration/expulsion in the microscopic devices. The superconductor is non-local, with large coherence length and weak pinning of flux. At lowest temperatures, behavior is dominated by screening currents that vary as a result of the temperature dependence of the magnetic penetration depth, modified by the effect of the non-uniformity of the applied field occurring on a scale comparable to the coherence length. In the temperature regime where responsivity is greatest, spatial variations in the order parameter become important: both local variations as flux enters/leaves the film and an intermediate state is formed, and globally as changing stability of the electrical circuit creates a Meissner transition and flux is expelled/penetrates to minimize free energy.

Magnetic Penetration Thermometer - Comparison with Metallic Magnetic Calorimeter

- Use temperature dependence of magnetic susceptibility of paramagnetic (Au:Er alloy) or diamagnetic (superconducting MoAu bilayer) film to sense temperature change in an x-ray absorber.
- MPT $d\phi/dT$ can be very large, e.g. larger than MMC

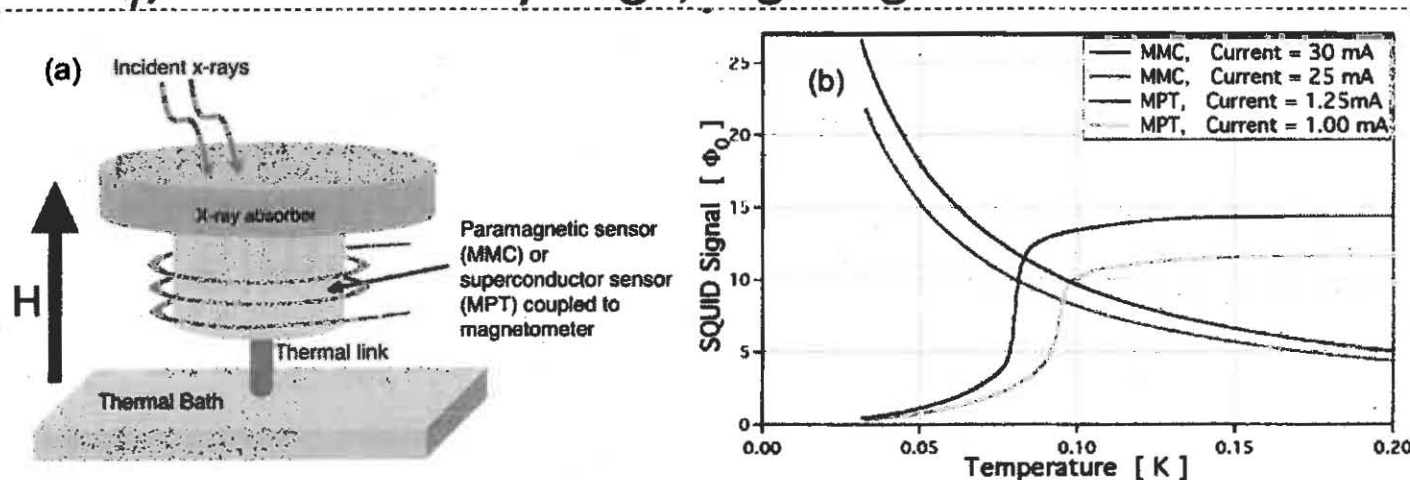
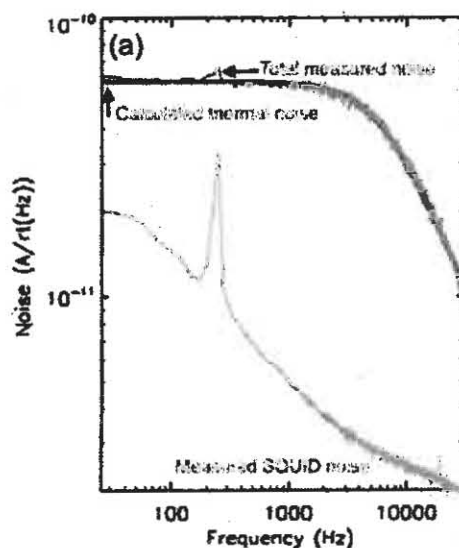


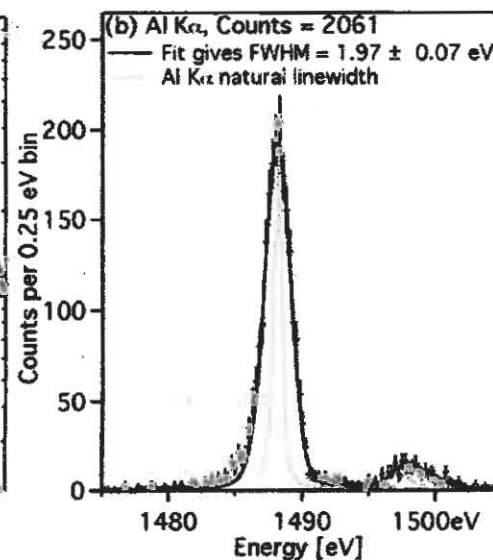
Figure 2: (Left) Basic schematic for both types of magnetically coupled microcalorimeters. (Right) Measured SQUID signal as a function of temperature for MMC and MPT microcalorimeters. The geometry of the pick-up loop and coupling to the SQUID is identical for these two types of detector. Two different curves generated by two different magnetic fields are shown for each sensor type.

Performance of MoAu MPT

- “Performance of Magnetic Penetration Thermometers for X-Ray Astronomy” by P. Nagler et al., *J. Low Temp. Physics*, 2012.
- Max $d\phi/dT \approx 1000 \Phi_0/K$; phonon & SQUID noise, no excess; achieved resolution = 2 eV FWHM at 1.5 keV; sub-eV possible



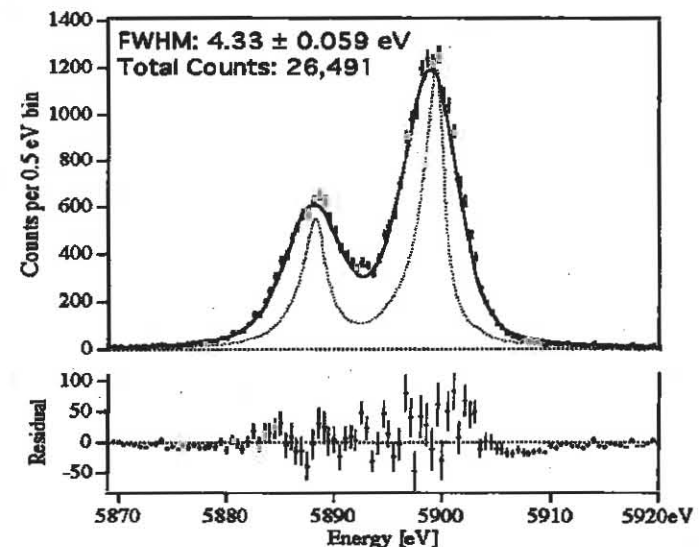
No absorber: phonon
+ SQUID noise only



BiAu absorber: 2eV @
1.5 keV (+ small tail)

ASC 2012 Portland

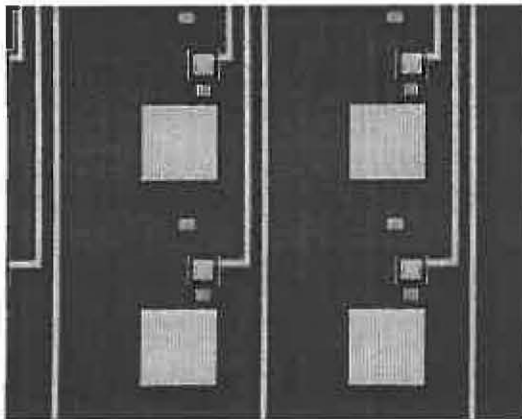
Histogram for $I_{\text{bias}} = 0.378$ mA and $T = 38.2$ mK



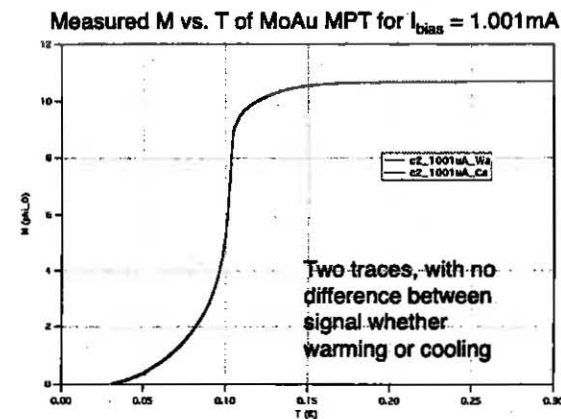
Au abs., 2nd batch T_c too low
($d\phi/dT \approx 20$): 4.3 eV @ 6keV
matches integrated NEP

Realization of Large ϕ - T Response

- MPTs from molybdenum-gold bilayers avoid flux penetration effects that reduced sensitivity of earlier Type-II hafnium devices, with low T_c for a high resolution microcalorimeter
- MoAu bilayer is a Type-I superconducting material, with large coherence length and weak pinning of flux



5x5 Pixel array with MoAu sensors

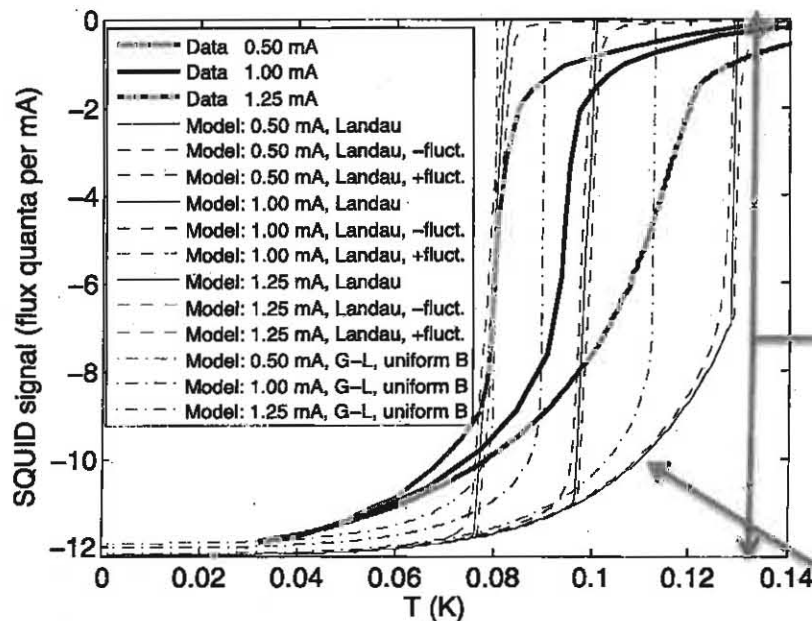


Large, non-hysteretic flux signal varies sensitively with temperature

Screening Currents

- screening currents (effective magnetic penetration depth)
 - MoAu is non-local; e.g. Sadleir found: $\lambda_0 = 0.079 \mu\text{m}$, $\xi_0 = 0.738 \mu\text{m}$, $T_c = 0.1709 \text{ K}$
 - Solve London equation with effective λ : $\lambda = \sqrt{\frac{m}{\mu_0 n q^2}}$ $\lambda_{\text{eff}} \approx (\lambda_L \xi_0^2)^{1/3}$

Measured and theoretical ϕ -T



- Numerical solution of London equation,

$$\nabla \times \mathbf{J} = \frac{1}{\mu_0 \lambda^2} \mathbf{B}$$

- gives J , B , L for λ :

- Overall $\Delta\phi$ sets $\lambda(0)$.

- T -dependence of λ ,

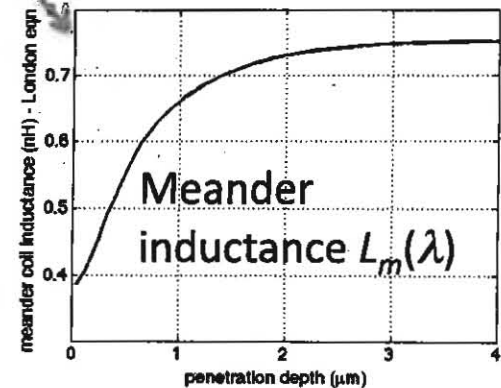
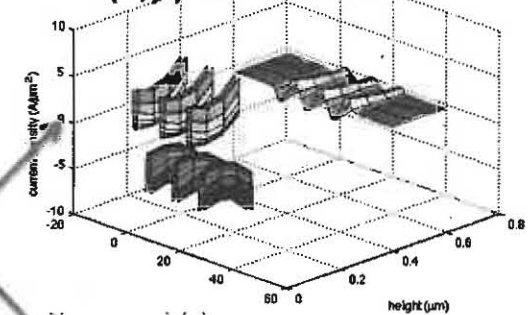
$$\lambda(T) \approx \frac{\lambda(0)}{\sqrt{1 - (T/T_c)^4}}$$

- predicts this curve for all bias currents.

ASC 2012 Portland

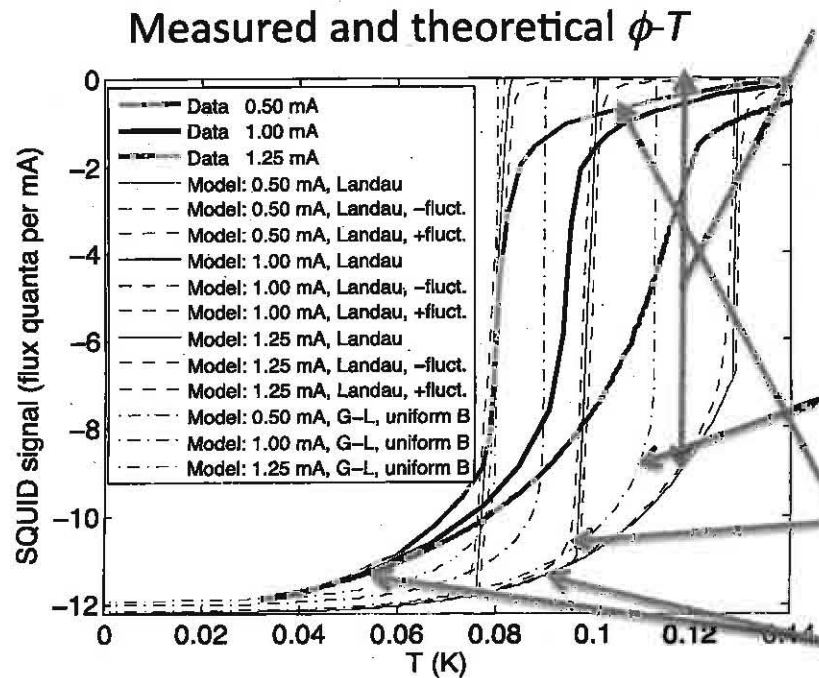
lambda = 0.16 μm , meander current = 1 A, dL/dmu0 = 0.15001 μH , $\mu_0 = 1.4943 \text{ A}\mu\text{m}^2$

$J(x,y)$ for $\lambda=160\text{nm}$



Meissner Effect

- Suppression of the order parameter to minimize free energy
 - F. London (1950): free energy normal/superc. (λ , Δ field independent)
 - G-L solution (Douglass, 1961): 2nd order transition if thin enough (seen in tunneling data)
 - Landau model w. bias circuit (minimize free energy for flux penetration in area fraction f)



• London: sudden drop to $\phi = 0$ from one curve.

• G-L has changing Δ :

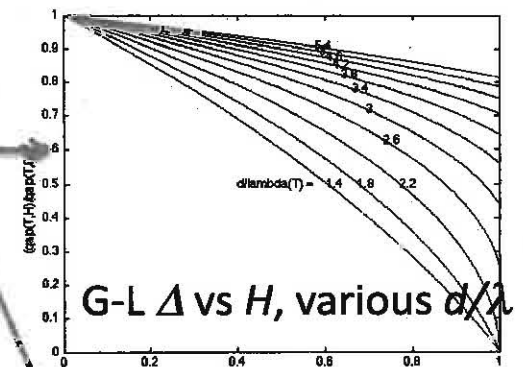
• G-L + self-consistent choice of λ ,

$$\frac{\lambda(T)}{\lambda(0)} = \left[\frac{\Delta(T)}{\Delta(0)} \tanh \frac{\Delta(T)}{2k_B T} \right]^{-1/3}$$

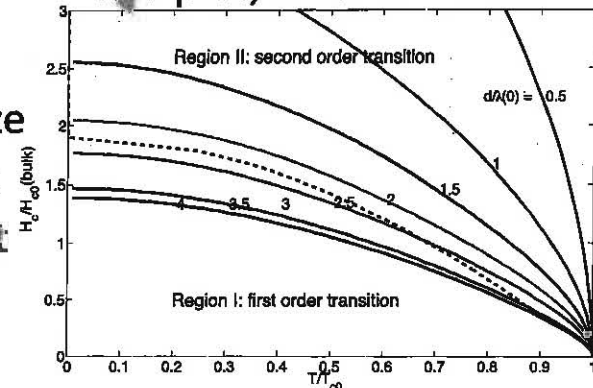
• predicts softened transition curves.

• Landau: predicts size of thermal rounding

• Discrepancy in limit curves at low T !

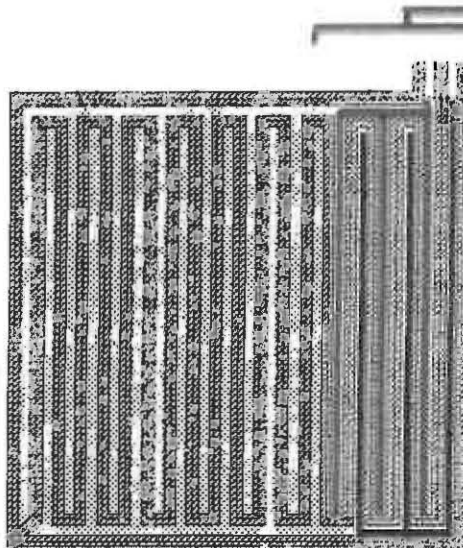


H - T plot, 1st or 2nd order



Landau Model with Bias Circuit

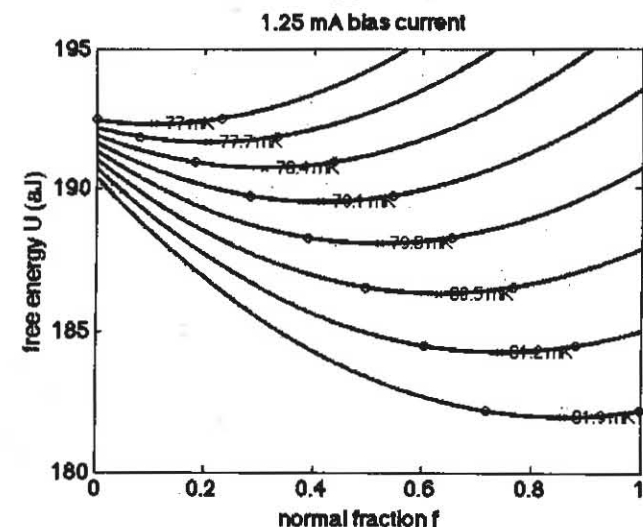
- Meander inductance L_m is in parallel with SQUID input (+ stray) L_i , and combination is in series with the large ballast inductor L_b .
- Region 1 = portion of sensor film that has expelled flux; Region 2 = stripes between meander traces where flux penetrates; f = fraction of Region 2
- Flux stays constant in niobium path thru L_m and L_i .
- Free energy includes interface energy: $U_{12} = (\xi_{GL}(T) - \lambda(T)) S \frac{B_{ch}^2(T)}{2\mu_0} = \left(\frac{1}{\kappa} - 1\right) \lambda(T) \frac{B_{ch}^2(T)}{2\mu_0} \frac{f 2s^2 d}{p}$
- If $L_i = 0$, then free energy is linear function of f , and f flips discontinuously between 0 and 1; if $L_i > 0$, then transition is broadened.
- Thermal fluctuations estimated from $\delta U = \sqrt{4k_B T^2 C}$



- Postulated region of intermediate state
- Almost all flux can be expelled (if bias < 1.25 mA for $T > 30$ mK)
- Edge barrier for fluxon escape to L_i must be small (also weak pinning)

ASC 2012 Portland

Free Energy vs f and T



Effect of Non-Uniform Applied Field

- Recall discrepancy: well below Meissner transition, ϕ should just reflect T -dependence of λ , but ϕ varies more at low T than expected from formulas for uniform applied field.
- BCS theory gives a wave vector dependent kernel $K(q)$ for the supercurrent J in response to an applied field:

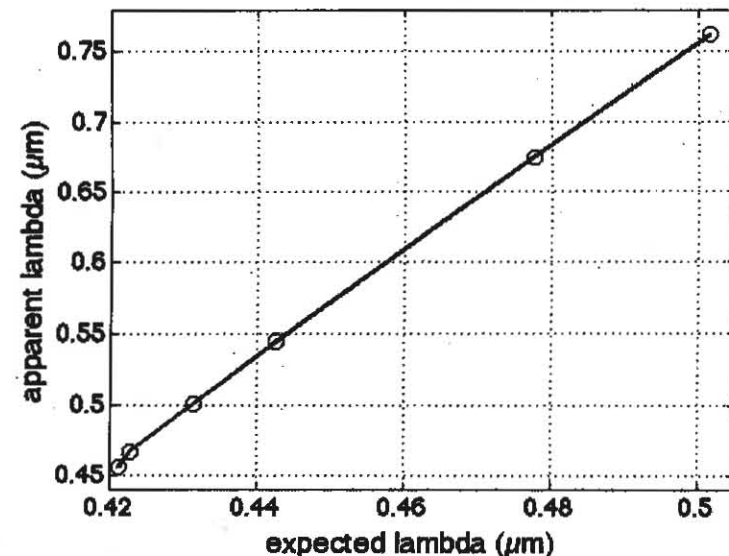
$$\mathbf{J} = -\mu_0 K(q) \mathbf{A}_{total} \quad \mu_0 [1 + q^2 / K(q)] \mathbf{J} = -q^2 \mathbf{A}_{applied} \quad K(0) = \frac{1}{\lambda^2}$$

- Our applied field has dominant wave vector $q = 2\pi/(2p)$, where $p = 5 \mu\text{m}$ is the meander pitch. Approximation for effective λ :

$$k(\mathbf{r}) \approx k(0)e^{-r/\xi_0} \Rightarrow K(q) \approx \frac{K(0)}{\left[1 + (q\xi_0)^2\right]^2} \quad \kappa = \frac{\lambda_L}{\xi_0}$$

$$\lambda_{eff} = \lambda_L \left[1 + (\xi_0 q)^2\right] = \lambda_L \left[1 + \left(\frac{\lambda_L}{\kappa}\right)^2 \left(\frac{2\pi}{2p}\right)^2\right]$$

- We observe an effect about the right size with plausible values $\lambda_L(0) = 0.20 \mu\text{m}$ and $\kappa \approx 0.1$

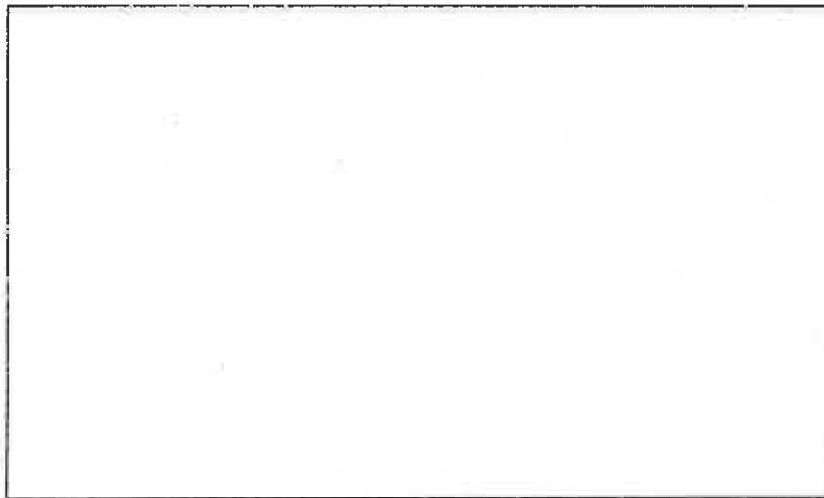


Meander Inductance from BCS Theory for Non-Uniform Applied Field

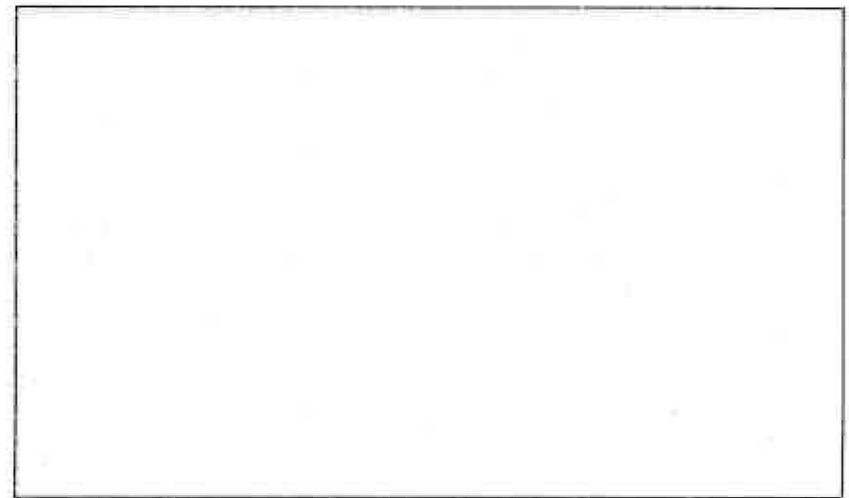
- BCS Kernel $K(q,T)$ gives the supercurrent response to vector potential A in Coulomb gauge
- Maxwell's equations relate A to sum of applied and response currents
- Solution method: Fourier expansion in x , find Green's function in z for $K = 0$, solve linear algebraic equation including K on z -grid
- Compute J , and magnetic and kinetic energies, to evaluate inductance per unit length

Use of BCS Inductance in $\phi - T$ models

- Fit low- T data with material parameters $\lambda_L(0)$ and ξ_0 to find inductance $L_m(T)$
- Use $L_m(T)$ in free energy of Landau model



Meander inductance versus temperature, calculated from BCS theory for our device geometry.



Landau model flux-temperature curves computed using BCS meander inductance.

Conclusions

- Like MMCs, MPTs enable high energy microcalorimeters with zero bias power dissipation and potential resolution < 1 eV
- MPTs can provide $d\phi/dT$ as large as $1000 \Phi_0/K$, with no excess noise, thereby reducing the importance of SQUID noise.
- Long coherence length in a Type-I superconducting MoAu film offers multiple advantages for efficient flux expulsion in MPT.
- Region of steepest $d\phi/dT$ is the Meissner effect in the small device; flux is expelled/penetrates to minimize free energy.
- Steepness of transition can be engineered with choice of film thickness and coil pitch relative to $\lambda_{\text{eff}}(0)$, ratio of T/T_c , and bias circuit inductance.

